Molecular Weight Dependence of Component Dynamics in Bidisperse Melt Rheology

Caroline M. Ylitalo, Julia A. Kornfield,† and Gerald G. Fuller*

Chemical Engineering Department, Stanford University, Stanford, California 94305-5025

Dale S. Pearson

Department of Chemical and Nuclear Engineering and Materials Department, University of California, Santa Barbara, California 93106

Received April 19, 1990; Revised Manuscript Received July 30, 1990

ABSTRACT: Simultaneous measurement of infrared dichroism and birefringence is used to study component relaxation in bimodal molecular weight distribution melts. Nearly monodisperse poly(ethylenepropylene) samples of molecular weights 53K, 125K, and 370K, all above the critical molecular weight for entanglement, were used. Results for the step-strain relaxation of each component and of the total sample are presented and discussed for binary blends of 10, 20, 30, 50, and 75% by volume of the higher molecular weight species for three sets of blends: 53K/125K, 53K/370K, and 125K/370K. For each sample, the relaxation dynamics of the blend and of each component depend upon the two polymer relaxation times and the blend composition. Effects of intermolecular orientational coupling interactions were observed, and a coupling strength of 0.45 was measured. The results of these experiments are compared to a reptation-based constraint release model, and a qualitative agreement is found.

1. Introduction

Polydispersity strongly affects the dynamics of polymer melts, and its influence on melt rheology has been the subject of many experimental investigations as well as theoretical studies. One simple, well-defined system used to examine the effects of polydispersity is a binary blend of well-characterized, monodisperse polymers. In such blends the relaxation dynamics are nonlinear functions of three independent parameters:[1] the molecular weight of the long polymer, M_L; the molecular weight of the short polymer, M_S; and the volume fraction of the long polymer, Φ_L. In a melt where both M_L and M_S are similar in magnitude and well above the critical molecular weight for entanglement of the polymer, reptation is expected to be the dominant mechanism of relaxation for both components, where each polymer chain is viewed to be confined by neighboring chains in a tubelike region with diameter equal to the average distance between entanglements.[2] This imaginary tube represents the effect of the uncrossable neighboring chains, which limit the lateral motion of the chain but allow its curvilinear diffusion along its mean contour.[3] As the difference between the two component molecular weights increases, the reptation times of the two polymers, τ_S and τ_L, become widely separated since they vary approximately as the cube of the polymer molecular weight, and the topological constraints surrounding the long chains no longer appear fixed. Therefore, an additional mode of relaxation becomes available to the long polymer by the release of short-chain constraints. Experimental evidence of this process[1] motivated the development of reptation-based theories that incorporate the effects of constraint release.[4-7]

In an earlier publication,[8] the relaxation dynamics following a step strain of binary blends of poly(ethylenepropylene) were studied. These blends had molecular weights M_S and M_L, both several times the entanglement molecular weight of the polymer. The relaxation curves observed for these blends were obtained by using a new rheooptical technique that allows the measurement of the total relaxation of a sample as well as the relaxation of each of the two components that make up the sample following a step strain. The strategy of this technique has been to optically label each component in the blend by replacing a portion of the hydrogens on the polymer backbone with deuterium and then perform measurements at the infrared wavelength of the carbon–deuterium stretching vibrational absorption.[8] Most of the relaxation features were qualitatively captured by current molecular models that incorporate constraint release, but a few experimental observations of component relaxations were not anticipated by any theories. The terminal long-chain relaxation was strongly influenced by the volume fraction of short chains in the blend, where increasing the short-chain concentration decreased the terminal relaxation time of the long chains. Another surprising feature was the significant retardation of the short-chain relaxation when long chains are present. It was proposed that this retardation is due to orientational coupling interactions between short-chain segments and the surrounding matrix. Although the strength of this interaction could not be calculated from the available data, an estimate of 30–40% was reported.[8]

The primary aim of this work has been to investigate the influence of variations in the molecular weights of the constituents of the blends by using the optical technique described above. Therefore, a new poly(ethylenepropylene) with a medium molecular weight (M_M) that lies in between the two molecular weights used in the previous study (M_S and M_L) is used. Each of the previous molecular weights is combined with this new polymer, and two sets of bidisperse blends are formed: M_S/M_M and M_M/M_L. For these new blends, reptation-based constraint release theories predict that the relaxation curves will be generally similar to those found in ref 8, but the features will be less pronounced due to the smaller difference in the two component molecular weights. However, this smaller difference allows the shape of the relaxation moduli at low concentrations of the longer component to cross from the box shape, where a distinct plateau is observed at times intermediate between the two component relaxation times,

* To whom correspondence should be addressed.
† Present address: Department of Chemical Engineering, California Institute of Technology, Pasadena, California 91125.

0024-9297/91/2224-0749$02.50/0

Table I
Properties of the Polymers Used

sample	MW	N	τ, s
S	53K	780	0.35
M	125K	1840	7
L	370K	5440	210

to the wedge shape, where no such plateau is expected.[9] Specifically, wedge-shaped moduli are predicted for the short/medium (S/M) blends for $\Phi_M < 0.18$ and for the medium/long (M/L) blends for $\Phi_L < 0.24$, whereas the short/long (S/L) blends are expected to have box-shaped relaxation moduli for all of the blend compositions studied.

Another goal of this work is to obtain a quantitative value for the strength of the observed intermolecular orientational coupling interactions, which could only be estimated from the previous results.[8]

The experimental methods employed in this work are described in the following section, while experimental results are given in section 3. In section 4, relaxation functions predicted by a current molecular model for these blends are compared with the experimental results, and the implications of this comparison are discussed in the concluding section.

2. Materials and Methods

A detailed description of the apparatus, signal possessing, and data collection along with polymer synthesis and characterization is given elsewhere;[8] however, a brief summary will be presented here in order to provide an appropriate background.

2.1. Polymer Synthesis and Characterization. The polymers used in these experiments are hydrogenated and deuteriated derivatives of polyisoprene, giving an exactly alternating ethylenepropylene polymer. For each polyisoprene derivative three degrees of polymerization are employed: short, medium, and long, with molecular weights 53 000, 125 000, and 370 000 respectively. These molecular weights together with the degree of polymerization, N, and the characteristic terminal relaxation time of each polymer are shown in Table I. Gel permeation chromatography, intrinsic viscosity measurements, and light scattering were used in molecular weight determination, and the reported values in Table I are the average of the molecular weights obtained from each method. It should be noted that for a given chain length (short, medium, or long), the hydrogenated and deuteriated polymers have identical degrees of polymerization, but the deuteriated polymers has a slightly higher molecular weight due to the heavier deuterium atoms.

The synthesis and characterization of the long and short chains were described earlier,[8] and the same methods were used for the medium polymer. The hydrogenated and deuteriated polymers of a given degree of polymerization have identical length, identical rheological properties, and negligible tendency toward phase separation. In addition, all six polyisoprene derivatives used in this study were anionically synthesized to produce almost monodisperse polymers ($M_w/M_n < 1.05$).[8]

2.2. Blend Preparation. The preparation of the blends used in this work follows the same technique reported in earlier experiments.[8] Two sets of blends were prepared: the first set was composed of short and medium chains and the second of medium and long chains. Five blend ratios were used: 10, 20, 30, 50, and 75% by volume longer polymer. For each blend ratio in each set, two samples were prepared: one containing 10% by volume deuteriated shorter chains and the other containing 10% by volume deuteriated longer chains. To each sample is added sufficient undeuteriated shorter and longer polymer to achieve the desired blend concentration. The optimal concentration of deuteriated polymer of 10% is dictated by the tradeoff between the transmitted light intensity and the dichroism: higher deuterium concentration decreases the intensity of the transmitted beam, and the lower deuterium concentration decreases the dichroism signal.

2.3. Experimental Method. Under flow conditions the state of stress of a sample gives rise to two optical properties: the birefringence, which is defined as the anisotropic retardation of light by the polymer, and the dichroism, which is defined as the anisotropic attenuation of light by the polymer. The birefringence is associated with the degree of segmental orientation and is proportional to the bulk state of stress according to the stress optical rule,[10] which was found to hold for thise blends by comparing birefringence data with relaxation modulus measurements.[8] On the other hand, the dichroism measures the segmental orientation of the labeled chains since it arises from the anisotropic absorption of light by the C–D bonds. This measure of the labeled component orientation can be interpreted in terms of the labeled chain contribution to the stress together with an orientational coupling between the labeled chains and the surrounding matrix.[11]

The optical apparatus used in these experiments has sufficient sensitivity for linear viscoelastic measurements, has a response time of 50 μs, and allows the simultaneous measurement of the transient dichroism and birefringence of a sample. A detailed description and a diagram of the optical train used is given elsewhere.[8] The light source is an infrared (IR) diode laser operating at the frequency of the C–D bond stretching vibrational absorption, 2190 cm^{-1}. The IR beam passes through a polarizer (oriented at 0°) and a photoelastic modulator (oriented at 45°) before impinging on the sample, which is held between two parallel windows in the flow cell. The flow cell used in these experiments has a parallel-plate geometry and 50–60-ms response time for step strains. A detailed description of its design can be found elsewhere.[12] The transmitted beam leaving the flow cell is first intercepted by a beam splitter (oriented at less than 5° with respect to the optical axis, so the polarization of neither beam is significantly changed); then it is observed by two separate detectors: the dichroism detector, which receives the transmitted beam, and the birefringence detector, which receives the reflected beam through a second polarizer oriented at −45°. Data acquisition and control of the step-strain experiments are accomplished by a microcomputer.

The light intensity at each detector is demodulated to determine the dichroism or the birefringence. The signal measured by each detector has the form

$$I = I_{DC} + I_{\omega} \sin(\omega t) + I_{2\omega} \cos(2\omega t) + \ldots \quad (2.1)$$

where ω is the photoelastic modulator frequency and it equals 84 kHz in these experiments. In an earlier work[8] it was found that the dichroism is proportional to $I_{2\omega}$ obtained at the dichroism detector, and the birefringence is proportional to I_{ω} obtained at the birefringence detector. The output from the dichroism detector is sent through a high-speed preamp to a lock-in amplifier set to a reference frequency of 2ω. Therefore, the output from this lock-in amplifier is $I_{2\omega}$, and it is proportional to the dichroism. Similarly, the output from the birefringence detector is aplified and sent to a lock-in amplifier set to a reference frequency of ω. Therefore, the output from this lock-in amplifier is I_{ω}, and it is proportional to the birefringence. The output from the two lock-in amplifiers and the signal from the displacement transducer on the flow cell are simultaneously recorded by using ans analog-to-digital converter.

The optical experiments were conducted in the same manner described for the S/L blends.[8] All experiments were performed at room temperature, and the reproducibility of the results was confirmed for each sample. For the S/M blends, sample thicknesses of 0.009–0.020 in. were used, and strains of 12–40% were applied. For the M/L blends, sample thicknesses of 0.012–0.020 in. were used, and strains of 12–30% were applied. In each case it was confirmed that the experiments were conducted in the linear viscoelastic regime by comparing results obtained with different strain magnitudes.

Following a step strain, the signals from both detectors show a rapid rise followed by a decay to the relaxation state base line. The signal from the dichroism detector is used to monitor the orientation of the labeled chains in the sample, and the signal from the birefringence detector is used to observe the state of stress of the bulk. The collected data for the dichroism have lower signal to noise ratios than the birefringence since the dichroism signal in these experiments is about 2 orders of magnitude smaller than the birefringence signal. At the end of each

experiment the thickness of the sample is measured directly by using a micrometer, and the signal from the displacement transducer together with the sample thickness is used to determine the exact magnitude of the strain.

The raw data were tabulated at logarithmically spaced time points (25 points/decade) and normalized by using the signal at 100 ms (the first reliable data point) as unity and the long-time base line as zero. Data collection in these experiments was started at t = 100 ms to allow for the mechanical response time of the flow cell (50–60 ms), and each reported data curve is the average of 32–60 experiments for the S/M blends and 18–35 experiments for the M/L blends. For each set of blends and at each volume fraction, optical measurements were performed on two samples: one with the shorter chains labeled and the other with the longer chains labeled. Then the birefringence data for the two samples were compared and found to agree in every case.

3. Results and Discussion

Through discussion of the results for the S/L blends is given elsewhere,[8] but these results are briefly repeated in this section (Figure 1) for comparison with the results for the S/M and M/L blends (Figures 2 and 3).

3.1. Bulk Relaxation. The birefringence data give a direct measure of the bulk relaxation for the blends since the stress optical rule is found to hold for the present polymer melts.[8] From comparison of Figures 1a, 2a, and 3a, it is clear that all three sets of blends exhibit certain general features; namely, as the matrix content of the longer chains is increased, the bulk relaxation is retarded. At short times bulk relaxation is due to two factors: shorter chain relaxation and a fast mode of the longer component relaxation afforded by the release of constraints imposed by the shorter chains in the matrix. At long times, however, bulk relaxation is goverened only by the longer chain relaxation as indicated by the shape of the relaxation curves. This is expected since the longest relaxation of the bulk is controlled by the slowest relaxing species in the blend.

When the relaxation times for all three polymers are considered, it is evident from Table I that $\tau_M = 20\tau_S$ and $\tau_L = 30\tau_M$, while $\tau_L = 600\tau_S$. Since $\tau_L/\tau_M \approx \tau_M/\tau_S$, it is expected that the stress relaxation curves for the M/L blends should be similar to those for the S/M blends but shifted in time. Since τ_L/τ_S is over 1 order of magnitude larger than τ_L/τ_M and τ_M/τ_S, the S/L blends are expected to give qualitatively sharper features due to the larger difference in the two component relaxation times. From bulk relaxation figures for the three blends, these expected features are clearly observed.

As discussed in the Introduction, theory[9] predicts that the S/L blends give box-shaped moduli with an intermediate plateau, a feature observed in the experimental results in Figure 1a. On the other hand, wedge-shaped moduli are predicted for the S/M blends at $\Phi_M = 0.1$ and for the M/L blends at $\Phi_L = 0.1$–0.2, while box shapes are predicted for the remaining curves. Experimental results, however, do not agree with these predictions where in Figures 2a and 3a all relaxation curves are wedge-shaped regardless of the blend composition.

3.2. Longer Component Relaxation. The dichroism data for samples with the longer component labeled provide a measure of the longer chain relaxation. Figures 1b, 2b, and 3b show these normalized relaxations for S/L, S/M, and M/L blends, respectively. For a given blend, the longer component relaxation is slower than that of the bulk, but the two are proportional at longer times because, as deduced from stress relaxation results, the longer component relaxation governs the long-time bulk relaxation.

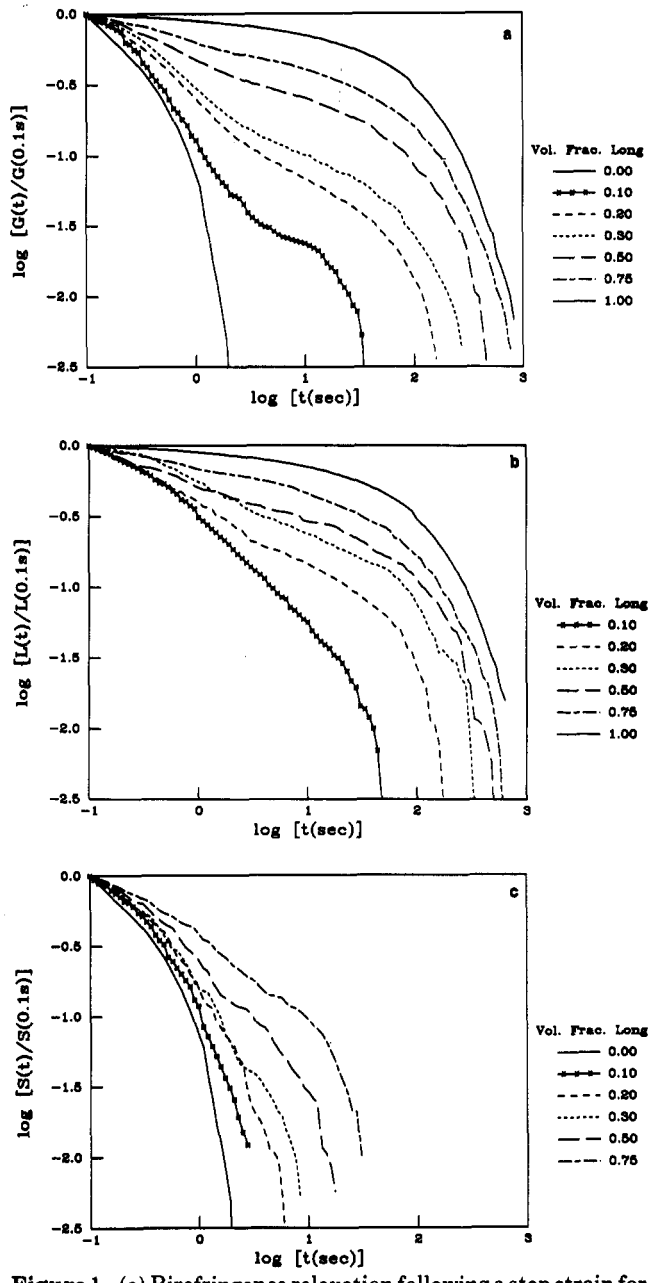

Figure 1. (a) Birefringence relaxation following a step strain for the S/L blends. (b) Long-chain dichroism relaxation following a step strain for the S/L blends. (c) Short-chain dichroism relaxation following a step strain for the S/L blends.

The results of our experiments indicate that the addition of shorter chains to the surrounding matrix strongly affects longer component relaxation curves as inferred from earlier studies.[1,8,13] With the addition of shorter chains, a fast mode of relaxation appears for the longer component, decreasing the magnitude of the long-time relaxation. This is attributed to the release of constraints imposed by the shorter chains that allows an additional mode of relaxation for the longer chains on the time scale of the shorter component relaxation. This fast relaxation leads to a decrease in the magnitude of the apparent long-time relaxation for the longer component as can be seen in Table II where the apparent longer component relaxation times for each blend are tablulated. For blends of 50% or greater by volume longer chains, the apparent longest relaxation time for the longer component is close to that of the monodisperse longer chains and its magnitude decreases linearly with decreasing Φ_L (Φ_M for the S/M blends). For blends with smaller longer chain volume fractions (less than 0.5), the apparent longest relaxation time of the longer

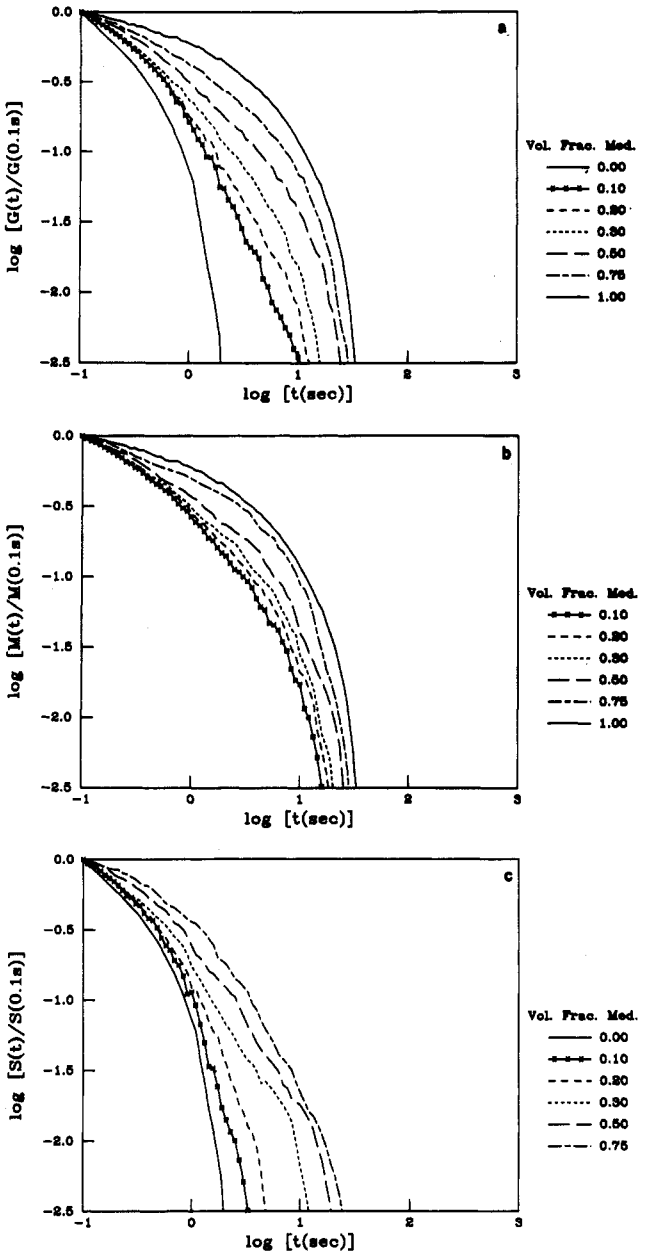

Figure 2. (a) Birefringence relaxation following a step strain for the S/M blends. (b) Medium-chain dichroism relaxation following a step strain for the S/M blends. (c) Short-chain dichroism relaxation following a step strain for the S/M blends.

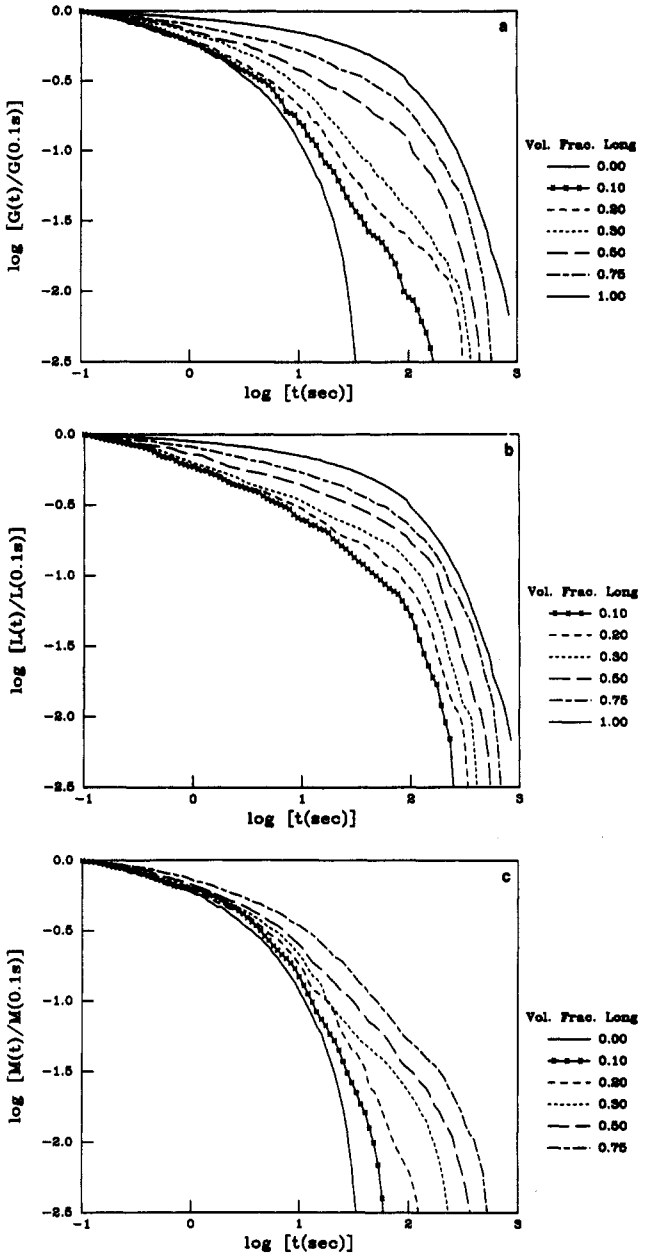

Figure 3. (a) Birefringence relaxation following a step strain for the M/L blends. (b) Long-chain dichroism relaxation following a step strain for the M/L blends. (c) Medium-chain dichroism relaxation following a step strain for the M/L blends.

chains decreases monotonically with their volumer fraction as is evident in Table II. The values for $\tau_{L,app}$ and $\tau_{M,app}$ in Table II were obtained from plotting the natural logarithm of the normalized relaxation moduli as a function of time and using the asymptotic slope for each curve to calculate the apparent relaxation times. These values for $\tau_{L,app}$ and $\tau_{M,app}$ are consistent with the longest relaxation times for the bulk as expected since the longer component in the blend controls its longest relaxation time.

All three longer component relaxation curves were closely examined at some intermediate time, τ, where

$$\tau = (\tau_i \tau_j)^{1/2} \tag{3.1}$$

and τ_i and τ_j are the shorter and longer component characteristic times, respectively. It was found that, at this time, the longer component relaxation increases linearly with shorter component volume fraction in all three blends, indicating an additive effect of constraint release at times shorter than the longer component relaxation time. These results are illustrated in Figure 4

Table II
Apparent Longest Relaxation Times (in seconds)

longer component volume fraction	S/L blends: $\tau_{L,app}$	S/M blends: $\tau_{M,app}$	M/L blends: $\tau_{L,app}$
0.10	20	2.8	50
0.20	60	3.5	70
0.30	120	4.5	130
0.50	150	6.4	160
0.75	180	6.7	186
1.00	210	7	210

where the normalized longer chain orientation at time τ is plotted as a function of its volume fraction in the blends. The symbols correspond to the experimental data, while the lines represent the best linear fit to the data points. For all three sets of blends the linear fits agree with the data within experimental error.

As shown in earlier work on the S/L blends,[8] for blends of less than 50% by volume longer chains, the longest relaxation time for the longer component significantly

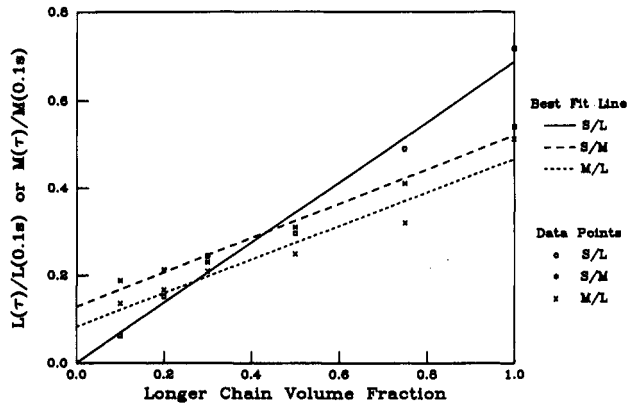

Figure 4. Normalized longer chain dichroism as a function of volume fraction at time $\tau = 9$ s (S/L blends), $\tau = 1.5$ (S/M blends), and $\tau = 36$ s (M/L blends).

decreases with increasing shorter chain concentration. In theory, this effect may be explained by tube dilation due to polydispersity, where the effective diameter of each tubelike region confining the longer chains becomes larger than it is in the pure longer component melt. This can occur if the lifetime of shorter component constraints imposed on the longer chains is on average shorter than the time required for a longer chain to diffuse a distance equal to the undilated tube diameter. However, the polymers used in these experiments do not obey the criterion for tube dilation since it was argued by Doi et al. that dilation of the idealized reptation tube can be ruled out if[9]

$$\frac{M_S^3}{M_e^2 M_L} \gg 1 \tag{3.2}$$

where M_e is the molecular weight between entanglements and equals 1800 for these polymers, and M_s and M_L are the shorter and longer component molecular weights, respectively. For all three blends $M_S^3/M_e^2M_L > 124$, so the shorter component is long enough to prevent tube dilation. Therefore, reptation controls the rate of diffusion of both species in a blend, and the longer chain diffusion rate becomes independent of matrix molecular weight.[14,15] In addition, it was explained by Doi et al. that, for blends that satisfy inequality (3.2), theory predicts that the terminal relaxation time of the longer chains is independent of blend composition and should be the same as that in a pure melt of longer polymer.[9] Therefore, there is no theoretical explanation for the experimentally observed decrease in the longer chain terminal relaxation time with decreasing its volume fraction in the melt.

The observed increase in longer component relaxation upon the addition of shorter chains is most evident in the S/L blends where, for low Φ_L, the terminal relaxation times for the long component are dramatically reduced. This effect is partly due to experimental error where data acquisition was terminated before total blend relaxation was reached, thereby introducing an error in base-line determination. Such an error has the effect of pulling down relaxation curves expecially when the measured magnitude of the orientation becomes small (at long times). Consequently, if data acquisition were extended, a lower base line would have been obtained, and experimentally determined relaxation curves would have been pulled upward and extended to longer times at the terminal region. This experimental error was eliminated with the S/M and M/L blends where data acquisition was extended for a long time. Therefore, the terminal relaxation time decrease for the longer chains with increasing shorter chain concentration cannot be explained in terms of experimental error alone; instead it can be due in part to orientational coupling interactions, which, if present in these blends, will have the effect of accelerating longer component terminal relaxation. The nature of these interactions and their effects will be discussed isn the following sections.

Table III
Times Required to Relax 99% (in Seconds)

	S/M blends		M/L blends	
longer chain volume fraction	t_{Bulk}	t_S	t_{Bulk}	t_M
0.10	5	3	76	48
0.20	9	4	250	75
0.30	11	9	275	190
0.50	18	15	370	300
0.75	22	17	530	430

3.3. Shorter Component Relaxation. Shorter chain relaxation is measured by the dichroism of samples with the shorter component labeled, and the results are presented in Figures 1c, 2c, and 3c for S/L, S/M, and M/L blends, respectively. In these figures the effect of longer chains in the matrix is surprisingly strong, producing a dramatic retardation in the shorter component relaxation with increasing concentration of longer chains. In Table III, the times required for the bulk and the shorter component to relax 99% of their initial orientation are tabulated for the S/M and M/L blends. When the bulk and shorter component relaxations are compared for the S/M and M/L blends, it is clear that, for longer component valume fractions between 0.3 and 0.75, the bulk and the shorter chains have proportional terminal relaxations, which suggest that shorter component orientation relaxes with the orientation in the surrounding matrix. (We infer that this conclusion is also true for smaller volume fractions of the longer component, but the dichroism signal is too small to measure.) For the S/L blends, the dichroism signal was not followed for sufficiently long times; therefore, no conclusive statements can be made regarding the terminal relaxation of the short chains for these blends.[8] For the shorter chains in a blend, reptation is the governing relaxation mechanism. Consequently, shorter component relaxation should remain virtually unchanged upon the addition of longer chains because the surrounding matrix appears fixed to the shorter chains regardless of the longer chains' concentration. In addition, experimental studies have shown that the diffusion coefficient of shorter chains into a matrix of longer chains is independent of matrix molecular weight for the molecular weights used in the present study.[14] Therefore, our experimental observations cannot be explained by the decrease in the diffusion coefficient of the shorter chains. Instead, we believe that this retarded relaxation is due to orientational coupling effects that can cause anisotropic orientation of the shorter chains on the length scale of chemical bonds, even when the orientation on the scale of a statistical reagent (of molecular weight M_e) has relaxed to an isotropic state. When a reptating shorter chain in an anisotropic matrix finds itself in an oriented mean field, its local orientation may be perturbed from its equilibrium conformation. Therefore, if orientational interactions exist in our blends, the terminal relaxation of the shorter chain dichroism (a measure of the local orientational distribution of C–D bonds in the blend) will be controlled by the bulk relaxation.

3.4. Short-Range Orientational Coupling. Orientational cooperativity in polymer melts can arise due to short-range forces acting on the segmental level. It was shown by Doi et al. that the strength of this interaction

can be measured by using the bulk and shorter component relaxations at times much greater than the reptation time of the shorter chains.[11] At such long times the following relationship holds[11]

$$(S/S_0) = \epsilon(G/G_0) \quad \text{for } t \gg \tau_s \tag{3.3}$$

where S/S_0 is the normalized shorter component relaxation, G/G_0 is the normalized bulk relaxation, and ϵ is the orientational coupling parameter and its magnitude is a measure of the strength of this coupling, where an ϵ value of one indicates complete coupling and a value of zero indicates no coupling. From (3.3) a plot of S/S_0 as a function of G/G_0 should be a straight line with a slope equal to ϵ.

A large body of experimental evidence[16-21] indicates that this coupling is effective at a very small length scale. Therefore, in our blends where the shortest polymer has a molecular weight that is several times the entanglement molecular weight, the orientational coupling coefficient, ϵ, is independent of molecular weight, and it is only a function of temperature[17,18] since all three polymers used in these experiments are identical in their microstructure. Consequently, it is expected that one would obtain the same value for ϵ from all three sets of blends and for all blend ratios.

The terminal relaxation of the S/M blends, shown in Figure 5, demonstrates the effects of orientation correlations where the normalized relaxation of the short chains is proportional to that of the bulk. From (3.3) one expectes all five lines in Figure 5 to meet at the origin. This holds for $\Phi_M = 0.3$–0.75, and we assume it holds for smaller volume fractions, but at very long times the dichroism becomes too small to measure. From the slopes of the lines in Figure 5, an average value of 0.45 ± 0.05 was determined for ϵ. For the other two series of blends (S/L and M/L), the results are consistent with $\epsilon \approx 0.45$ but are subject to poorer signal to noise ratios. This value for ϵ is within the range of reported values in literature, which vary between 0.26 and 1.0[16-18,20-23] for a variety of systems that include small molecules embedded in stretched polymer films or networks,[17,18,20] oligomers in polymer networks,[16,21] stretched films of isotopically labeled block copolymers,[22] and short unentangled polymer chains in a matrix of long entangled chains.[23] The techniques used in those measurements include deuterium NMR spectroscopy,[16,17,21] IR dichroism,[20,22,23] and UV–vis dichroism.[18] A critical comparison among all these systems is beyond the scope of this paper, but a detailed review and additional experimental results will be presented in a future publication.[24]

4. Model Calculations

In this section we compare the measured bulk and component relaxation curves to the predictions of a reptation-based constraint release model. Various models that incorporate constraint release into the theory of reptation are present in literature,[4-7,25-27] and a comparison among them is given by Rubinstein et al.[5] For comparison with our results, we selected the Rubinstein–Helfand–Pearson (RHP) model[5] for two reasons: first, it does not postulate tube dilation,[6,7,9] a phenomenon not present in our blends, and, second, it uses only two parameters, the plateau modulus, G_N°, and the medium-component relaxation time, τ_M, both readily available from linear viscoelastic data on the pure medium polymer. (Actually, this model requires a third parameter, κ, which is the ratio of the characteristic waiting time for a constraint release event to the characteristic reptation time. For these

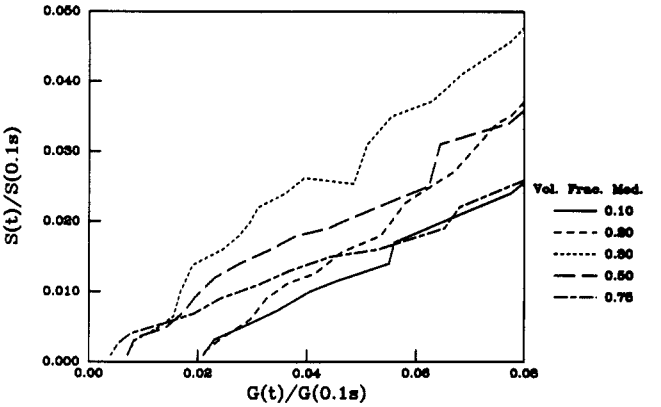

Figure 5. Normalized shorter chain dichroism as a function of normalized birefringence relaxation in the terminal relaxation region for the S/M blends. The slope of the lines equals the orientational coupling coefficient, ϵ.

calculations, however, this parameter is set equal to one.)[28] In addition, orientation correlation effects are incorporated into the RHP model so that a more accurate comparison can be made between our experimental data and the theoretical predictions.

There exist two independent, equally convincing theories to model orientational coupling effects on the relaxation dynamics of oriented polymer melts. The first model, developed by Merrill et al.,[29] involves modification of the basic reptation model proposed by Doi and Edwards for configurational and stress relaxations.[2] This modification consists of removing the assumption that relaxing segments that emerge from the oriented tubes adopt random, isotropic configurations and adding a boundary condition that restricts the available configurations for these segments. As a result, emerging segments from the ends of the stressed tubes are affected by the orientation of the surrounding matrix and, to a certain extent, align with it. Therefore, this is a boundary value, self-consistent, mean-field treatment. On the other hand, a second model for orientational coupling, developed by Doi et al.,[11] considers the orientation of a polymer segment in a melt to be equal to the sum of two values: the orientation of the primitive path or reptation tube and a certain percentage, given by ϵ (the magnitude of the coupling), of the average matrix orientation leading to a self-consistent, mean-field treatment for the problem.

The fundamental difference between the two models can be summarized as follows. Merrill et al. do not make a distinction between the local orientation on the length scale of the chemical bonds and that on the scale of statistical segments, and they propose that orientation correlations produce anisotropy on the statistical segment level, while Doi et al. propose that orientational coupling interactions produce anisotropy on the chemical bond level but not on the statistical segment level. Until now, however, there is nso clear evidence to indicate which assumption is correct. In the following theoretical calculations, we will restrict our attention to the model proposed by Doi et al.

4.1. Rubinstein–Helfand–Pearson Model. The RHP model describes thes stress relaxation of a blend as the result of two independent mechanisms: reptation, by which the stressed chain disengages from the deformed tube, and constraint release, by which the deformed tube relaxes. In fully entangled bidisperse melts, the reptation of both species is independent of constraint release if the short-chain constraints have a lifetime that is longer than the time needed for a long chain to diffuse between

two successive entanglements.[9] In addition, diffusion results indicate that the criterion for reptation and constraint release to be independent is[15]

$$\frac{M_S^3}{M_e^2 M_L} \gg 10 \tag{4.1}$$

For the polymers used in the present experiments, this ratio is greater than 124. Consequently, reptation and constraint release can be assumed independent and the RHP model can be applied.

According to the theory of reptation, each polymer chain is confined by neighboring chains inside an imaginary tube, which will be perturbed from its equilibrium conformation and deformed under the influence of external stresses. When this effective tube is deformed, the terminal relaxation of the stressed chain confined in it is controlled by curvilinear diffusion that allows the chain to escape from the stressed tube.[2] The time dependence of chain relaxation is governed by the one-dimensional diffusion problem for the first passage of a chain end out of a portion of the initial tube.[3] The solution to this problem gives the fraction of the initial tube remaining at time t as

$$\mu(t/\tau) = \frac{8}{\pi^2} \sum_{p \text{ odd}} \frac{1}{p^2} e^{-p^2 t/\tau} \tag{4.2}$$

where μ is the remaining fraction of the tube, and τ is the characteristic time for the polymer chain to complete departure from the tube. On the other hand, the concept of constraint release incorporates the effects of polydispersity, where the motion of shorter chains changes the conformation of the tube and allows the partial relaxation of sections of it, thereby reducing its effectiveness. For simplicity, in the remaining of this section the labels S and L will denote the shorter and longer components of an arbitrary binary blend.

The RHP model gives the relaxing memory function, F_K, for a given blend component as the product of the remaining fraction of the tube, μ, and its relative effectiveness, R

$$F_K(t) = R(t)\, \mu(t/\tau_K) \tag{4.3}$$

where the subscript K is S or L depending on the length of the polymer chains described. The matrix function R is taken to have a slow mode with a characteristic time determined by the reptation time of the long chains, τ_L, and a fast mode with a characteristic time τ_S. The magnitude of these two modes is assumed to be proportional to the volume fractions of the long and short components:

$$R(t) = \Phi_L \Theta(t/\tau_L) + \Phi_S \Theta(t/\tau_S) \tag{4.4}$$

In the present calculations, we used an approximate form of the Rouse relaxation spectrum for the function Θ given by[28]

$$\Theta(t) = \exp(-4t/\tau) I_0(4t/\tau) \tag{4.5}$$

where I_0 is the zeroth-order modified Bessel function. In order to arrive at this final form of the relaxation function, several assumptions and approximations were made, all of which are discussed in another publication.[28]

The bulk relaxation modulus, $G(t)$, is given by

$$G(t) = G_N^0[\Phi_L F_L(t) + \Phi_S F_S(t)] \tag{4.6}$$

or, in terms of component contributions, the relaxation modulus can be written as

$$G(t) = \Phi_L L(t) + \Phi_S S(t) \tag{4.7}$$

where $L(t) = G_N^0 F_L(t)$ and $S(t) = G_N^0 F_S(t)$ are the long- and short-component relaxation moduli in a given blend.

Because orientation correlations are evident in the experimental results, it is desirable to incorporate their effects into the RHP model so that the theoretical calculations are more realistic in representing blend behavior. As discussed in the previous section, the model proposed by Doi et al.[11] will be used in the following analysis. (Note that this analysis or orientational coupling interactions is model independent and is readily incorporated into the RHP model.) On the basis of the experimental results, an orientational coupling constant of $\epsilon = 0.45$ is used to obtain model predictions for the component orientational relaxation functions:

$$L_{oc}(t) = (1 - \epsilon)L(t) + \epsilon G(t) \tag{4.8}$$

and

$$S_{oc}(t) = (1 - \epsilon)S(t) + \epsilon G(t) \tag{4.9}$$

These relaxation functions are used in this section, but a comparison between model predictions with and without orientational coupling is discussed in the appendix.

To minimize thes number of parameters used in the calculations, the long- and short-component relaxation times are written in terms of the medium polymer relaxation time using the theory of reptation prediction that the relaxation time of a polymer is proportional to the cube of its molecular weight:

$$\tau_L = (M_L/M_M)^3 \tau_M \tag{4.10}$$

and

$$\tau_S = (M_S/M_M)^3 \tau_M \tag{4.11}$$

Experimentally, this exponent was found to be 3.4,[30] but the prediction of the reptation theory was used for the sake of consistency in our calculations, which are based primarily on the theory of reptation. Using an exponent of 3 in the calculations resulted in slightly different relaxation times for the short and long polymers in the model than in actuality; therefore, the predicted relaxation functions for the pure components are slightly shifted from the experimental ones.

The following three sections compare model predictions to experimental results. In order to achieve the desired comparisons, all model predictions are normalized by the corresponding values at $t = 100$ ms, which is the starting time for data collection in our experiments after allowing for the mechanical response time of the apparatus.

4.2. Model Predictions for the Bulk. The predicted bulk relaxation functions for the three sets of blends were calculated from (4.6), and the normalized results are given in Figures 6a and 7a. Comparison of these graphs with the experimental results in part a of Figures 1–3 indicates that the RHP model captures the general trends of bulk relaxation and gives good qualitative agreement for all three sets. The lack of extract quantitative agreement is mostly due to the use of 3 for the exponent in (4.10) and (4.11), which resulted in shorter relaxation time for the long polymer and longer relaxation time for the short polymer.

It is interesting to note that the predicted shapes for the stress relaxation curves agree with the experimental observations: the S/L blends have box-shaped relaxation curves and the S/M and M/L blends have wedge-shaped

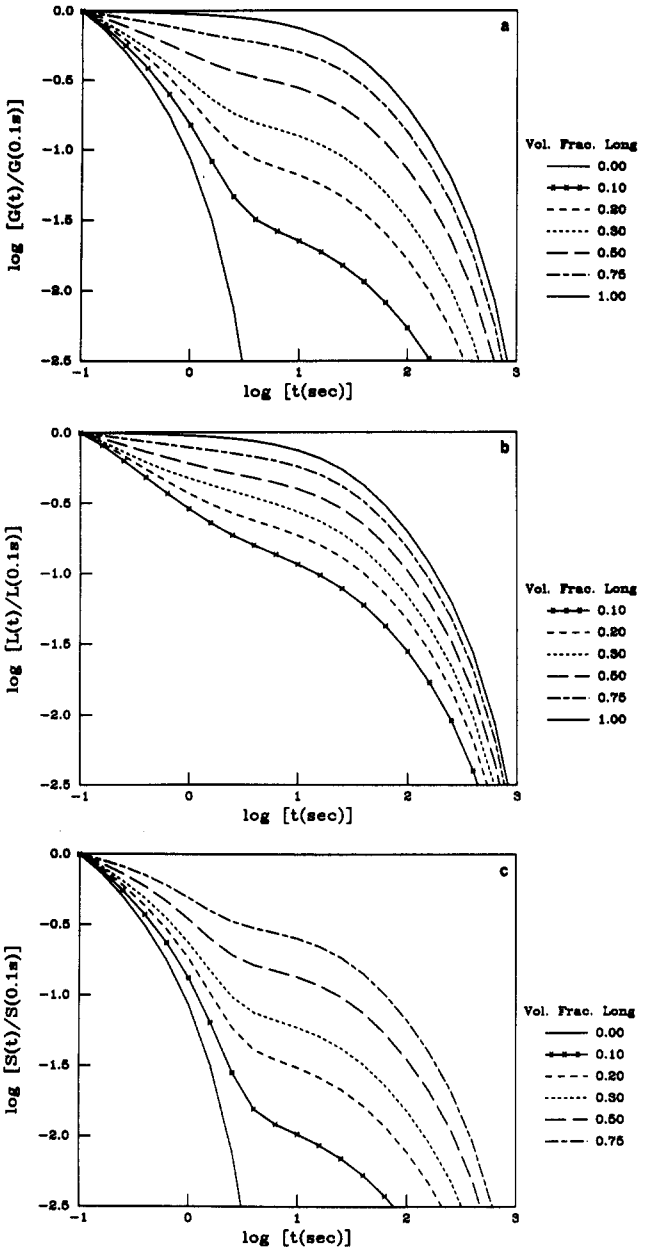

Figure 6. (a) RHP model predictions for the normalized stress relaxation following a step strain (S/L blends). (b) RHP model predictions for the normalized long-chain relaxation following a step strain with orientational coupling parameter $\epsilon = 0.45$ (S/L blends). (c) RHP model predictions for the normalized short-chain relaxation following a step strain with orientational coupling parameter $\epsilon = 0.45$ (S/L blends).

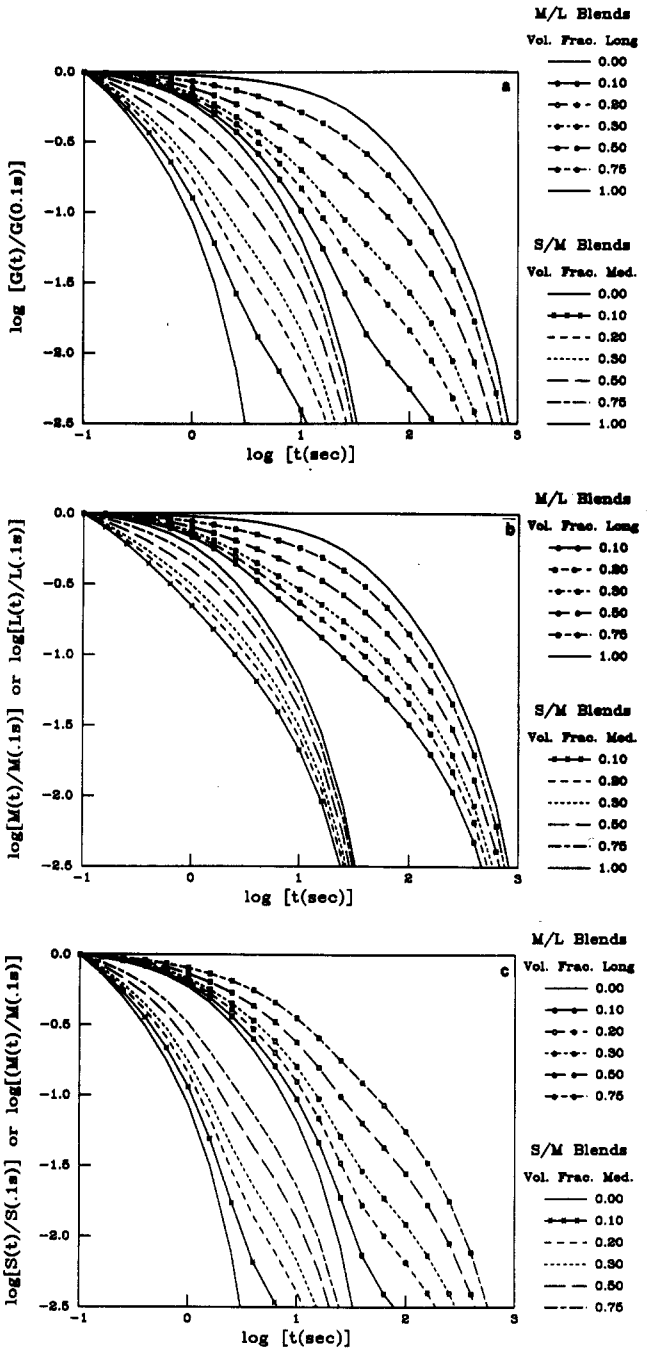

Figure 7. (a) RHP model predictions for the normalized stress relaxation following a step strain (S/M and M/L blends). (b) RHP model predictions for the normalized longer chain relaxation following a step strain with orientational coupling parameter $\epsilon = 0.45$ (S/M and M/L blends). (c) RHP model predictions for the normalized shorter chain relaxation following a step strain with orientational coupling parameter $\epsilon = 0.45$ (S/M and M/L blends).

relaxation curves for all blend compositions. These observations disagree with the predictions of Doi et al., which were discussed in the section 3.1.[9]

4.3. Model Predictions for the Longer Component. The RHP model predictions for the longer component relaxation after incorporating the effects of orientational coupling interactions with $\epsilon = 0.45$ were calculated from (4.8). These results are shown in part b of Figures 6 and 7. Comparison of these theoretical predictions to experimental results in part b of Figures 1–3 indicates that, although most of the qualitative features are captured by the model, such as the increased relaxation at short times due to constraint release leading to shorter overall relaxation time, the agreement is not quantitative. For all three blends, the most pronounced discrepancy is seen at longer times where theory predicts that, in the absence of tube dilation, terminal relaxation of the longer chains should approach that of the pure longer component more closely than is actually observed. When the predicted normalized orientation of the longer chains at time T [from (3.1)] is plotted as a function of the longer chain volume fraction, a straight line is obtained for the S/L and S/M blends as shown in Figure 8. For the M/L blends the resulting plot has a small positive curvature. Although experimental results for all three sets of blends gave straight lines in Figure 4, the scattering of experimental data for the M/L blends makes it difficult to judge if the data represent a straight line or a slightly curved one as predicted by the RHP model.

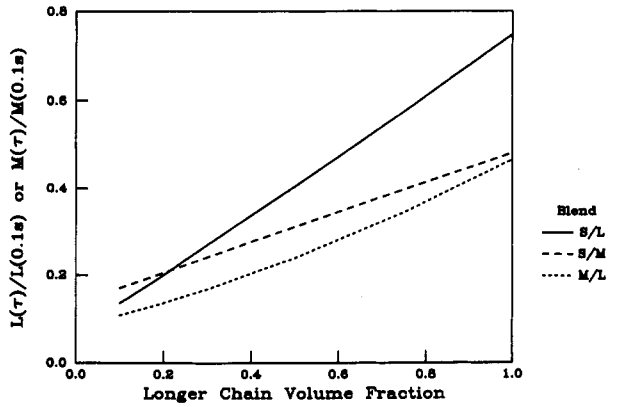

Figure 8. RHP model predictions for the normalized longer chain relaxation as a function of volume fraction at time $\tau = 9$ s (S/L blends), $\tau = 1.5$ s (S/M blends), and $\tau = 36$ s (M/L blends).

4.4. Model Predictions for the Shorter Component. The RHP model predictions for the shorter component relaxation were obtained from (4.9) with an orientational coupling constant $\epsilon = 0.45$. These predictions are given in Figures 6c and 7c. Comparison of these results to experimental curves in part c of Figures 1–3 indicates that there is a good agreement between theory and experiment for the S/M and M/L blends. While the S/L blends show vast differences at long times, this disagreement is mostly due to the lack of experimental data for the short-component relaxation at long times. Clearly this good agreement between theory and experiment for the S/M and M/L blends supports the assumption that orientation correlations influence bond orientation in these blends. Without orientational coupling interactions, model predictions for the shorter component do not resemble the experimental results as shown in the Appendix (Figure 9).

5. Conclusions

A rheooptical technique that allows simultaneous measurement of bulk and component relaxations is used to study bidisperse polymer melts. Three polymers designated as short (S), medium (M), and long (L) with sharply defined molecular weights were used to construct three sets of blends: S/L, S/M, and M/L. Results of step-strain relaxation experiments on samples containing different volume fractions of the longer chains show that all three sets of blends exhibit similar behavior both for the bulk and the individual components.

The retardation in the shorter component relaxation in all three blends is considered as evidence or orientational coupling interactions, and a coupling parameter of 0.45 was measured from experimental results for the S/M blends.

As the shorter component concentration is increased in the blends, the longer component relaxation curves are changed. There is an increase in short-time relaxation, which is afforded by the release of constraints imposed by the shorter chains. Also, there is a decrease in the longest relaxation times, which is due in part to orientational coupling effects, but the major cause of this observation is not yet understood.

In addition, the RHP model, a reptation-based constraint release model, was used to predict bulk and component relaxations for these blends. From comparison with experiment, it was concluded that, although most of the qualitative features of the experimental results were captured by the RHP model, some discrepancies exist. The major difference was evident in the longer chain relaxation where the experimentally observed decrease in the terminal relaxation time for the longer component is not fully accounted for by the model even after including orientational coupling effects. This observation has no theoretical explanation; it may be due to additional cooperativity in relaxation, which would require a self-consistent mean-field treatment.

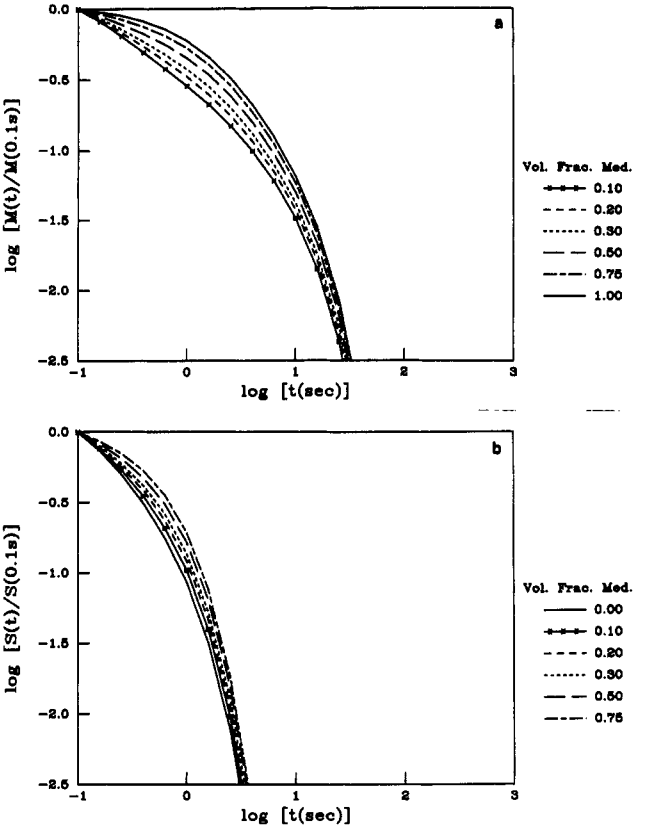

Figure 9. (a) RHP model predictions for the normalized medium-chain relaxation following a step strain without orientational coupling (S/M blends). (b) RHP model predictions for the normalized short-chain relaxation following a step strain without orientational coupling (S/M blends).

Acknowledgment. We are grateful to the National Science Foundation for support through the Presidential Young Investigator program for G. Fuller. This work was also supported by the Exxon Foundation and the Center for Materials Research at Stanford University. We thank Lewis Fetters for synthesizing the polymers used in this study.

Appendix: Comparison of Model Predictions with and without Orientational Coupling

In order to emphasize the influence of orientational coupling, relaxation curves calculated without its incorporation are presented and compared to the corresponding results with orientational coupling effects. Since the relaxation functions without orientational coupling were similar for all three blends, only the predictions for the S/M blends are presented.

Model predictions for the longer component stress relaxation without including orientational coupling effects are shown in Figure 9a for the S/M blends. From comparison of these curves to model predictions that include orientational coupling in Figure 7b, it can be concluded that orientational coupling interactions slightly accelerate longer component orientational relaxation, leading to a decreased overall relaxation time.

Similarly, shorter component stress relaxations without orientational coupling are shown in Figure 9b for the S/M

blends. Comparison with Figure 7c clearly shows the effect of orientational coupling because the relaxation curves in Figure 9b do not remotely resemble the corresponding experimental observations in Figure 2c. Without orientational coupling, the RHP model predicts that the shorter component orientational relaxation is only slightly affected by longer chain concentration, a consequence of the theory of reptation.

References and Notes

(1) Struglinski, M. J.; Graessley, W. W. *Macromolecules* **1985**, *18*, 2630.
(2) Doi, M.; Edwards, S. F. *J. Chem. Soc., Faraday Trans. 2* **1978**, *74*, 1789, 1802, 1818.
(3) de Gennes, P.-G. *J. Chem. Phys.* **1971**, *55*, 572.
(4) Graessley, W. W. Entangled Linear, Branched and Network Polymer Systems—Molecular Theories. *Adv. Polym. Sci.* **1982**, *47*, 67.
(5) Rubinstein, M.; Helfand, E.; Pearson, D. S. *Macromolecules* **1987**, *20*, 822.
(6) Marrucci, M. *J. Polym. Sci., Polyym. Phys. Ed.* **1985**, 23, 159.
(7) Viovy, J. L. *J. Phys. (Les Ulis., Fr.)* **1985**, *46*, 847.
(8) Kornfield, J. A.; Fuller, G. G.; Pearson, D. S. *Macromolecules* **1989**, *22*, 1334.
(9) Doi, M.; Graessley, W. W.; Helfand, E.; Pearson, D. S. *Macromolecules* **1987**, *20*, 1900.
(10) Janeschitz-Kriegl, H. *Polymer Melt Rheology and Flow Birefringence*; Springer-Verlag: New York, 1983.
(11) Doi, M.; Pearson, D. S.; Kornfield, J.; Fuller, G. G. *Macromolecules* **1989**, *22*, 1488.
(12) Kornfield, J. A.; Fuller, G. G.; Pearson, D. S. *Rheol. Acta* **1990**, *29*, 105.
(13) Montfort, J. P.; Marin, G.; Monge, D. *Macromolecules* **1984**, *17*, 1551.
(14) Green, P. F.; Mills, P. J.; Palmstrom, C. J.; Mayer, J. W.; Kramer, E. J. *Phys. Rev. Lett.* **1984**, *53*, 2143.
(15) Green, P. F.; Kramer, E. J. *Macromolecules* **1986**, *19*, 1108.
(16) Sotta, P.; Deloche, B.; Herz, J.; Lapp, A.; Durand, D.; Rabadeux, J.-C. *Macromolecules* **1987**, *20*, 2769.
(17) Deloche, B.; Samulski, E. T. *Macromolecules* **1981**, *14*, 575.
(18) Thulstrup, E. W.; Michl, J. *J. Am. Chem.* **1982**, *104*, 5594.
(19) Michl, J.; Thulstrup, E. W. *Spectroscopy with Polarized Light*; VCH Publishers, Inc.: New York, 1986.
(20) Schmidt, P.; Schneider, B. *Makromol. Chem.* **1983**, *184*, 2075.
(21) Jacobi, M.; Stadler, R.; Gronski, W. *Macromolecules* **1986**, *19*, 2884.
(22) Tassin, J. F.; Monnerie, L.; Fetters, L. J. *Macromolecules* **1988**, *21*, 2404.
(23) Tassin, J. F.; Baschwitz, A.; Moise, J. Y.; Monnerie, L. *Macromolecules* **1990**, *23*, 1879.
(24) Ylitalo, C. M.; Fuller, G. G.; Abetz, V.; Stadler, R. Oligomers as Molecular Probes of Orientational Coupling Interactions in Polymer Melts. In preparation.
(25) Daoud, M.; de Gennes, P.-G. *J. Polym. Sci. Polym. Phys. Ed.* **1979**, *17*, 1971.
(26) Rubinstein, M.; Colby, R. H. *J. Chem. Phys.* **1988**, *89*, 5291.
(27) Watanabe, H.; Tirrell, M. *Macromolecules* **1988**, *22*, 927.
(28) Kornfield, J. A.; Fuller, G. G.; Pearson, D. S. Third Normal Stress Difference and Component Relaxation Spectra for Bidisperse Melts under Oscillatory Sheat. Submitted for publication in *Macromolecules*.
(29) Merrill, W. W.; Tirrell, M.; Tassin, J.-F.; Monnerie, L. *Macromolecules* **1989**, *22*, 896.
(30) Larson, R. G. *Constitutive Equations for Polymer Melts and Solutions*; Butterworths: Boston, 1988.